Journal of High Energy Physics, Gravitation and Cosmology, 2024, 10, 693-709
https://www.scirp.org/journal/jhepgc
ISSN Online: 2380-4335
ISSN Print: 2380-4327

Life Origin in the Milky Way Galaxy: III. Spatial Distribution of Overheated Stars in the Solar Neighborhood

Alexander N. Safronov

Obukhov Institute of Atmospheric Physics, Russian Academy of Sciences, Moscow, Russia
Email: safronov_2003@mail.ru

How to cite this paper: Safronov, A.N. (2024) Life Origin in the Milky Way Galaxy: III. Spatial Distribution of Overheated Stars in the Solar Neighborhood. *Journal of High Energy Physics, Gravitation and Cosmology*, **10**, 693-709.
https://doi.org/10.4236/jhepgc.2024.102042

Received: January 19, 2024
Accepted: April 7, 2024
Published: April 10, 2024

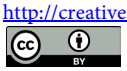

Abstract

A concept of ensemble averaged stellar reactors is developed to study the dynamics of processes occurring in stars, allocated in the ~200 pc solar neighborhood. According to the effective temperature value, four stellar classes are identified, for which the correlation coefficients and standard deviation are counted. The theory of the buoyancy terrestial elements is generalized to stellar systems. It was suggested that stars are over-heated due to the shift parameters of the nuclear processes occurring inside the stars, which leads to the synthesis of transuranium elements until the achievement of a critical nuclear mass and star explosion. The heavy transuranium elements sink downward and are concentrated in the stellar depth layers. The physical explanation of the existence of the critical Chandrasekhar star limit has been offered. Based on the spatial analysis of overheated stars, it was suggested that the withdrawal of the stellar reactor from the equilibrium state is a consequence of extragalactic compression inside the galaxy arm due to the arm spirality (not to be confused with the spirality of the galaxy itself).

Keywords

Stellar Nucleogenesis, Ensemble-Averaged Stellar Reactor, Overheated Stars, Chandrasekhar Stellar Limit, Arm Spirality

1. Introduction

In astrophysics, stellar nucleosynthesis has been studied thoroughly for an extended period. Briefly, we recall the history of stellar nucleosynthesis. In 1946, Hoyle suggested that elements, up to iron and nickel, could be synthesized in stars [1] [2]. As it is known to explain the origin of elements heavier than iron, the theory of the generation of chemical elements was extended, and in the

theory, it was added the slow and rapid processes of neutron capture (s- and r-processes) by [3]. Below this theory was called as B^{2}FH model or theory. Usually, the s- and r-processes occurred inside massive stars or during explosive and catastrophic events, such as merging Neutron Star (mNS) or core-collapse Super Novae (ccSNe). More details about nucleosynthesis of the chemical elements during s- and r-process could be found in several studies [4]-[15] and many others.

Recently [16] was published a new concept about the element nucleosynthesis. In the Kobayashi et al. model (below K^{2}L) it was performed the construct a new GCE model for all stable elements from carbon (A = 12) to uranium (A = 238) from first principles, *i.e.*, by using theoretical nucleosynthesis yields and event rates of all chemical enrichment sources.

In the B^{2}FH model, the frequency of neutron star collisions raised doubts, so we consider a new K^{2}L model. According to the K^{2}L model, the neutron star collisions do not create the quantity of chemical elements than previously assumed. However this K^{2}L model can not explain the number of such elements as Cl, K, Sc, As, and Au and creates a new astronomical *mystery*. The new K^{2}L mode did not solve the previous B^{2}FH model's problems.

In previous work [17], we presented a fairly sufficiently detailed discussion to justify the failure of the B^{2}FH and K^{2}L models. In particular, in [17], it is discussed such paradoxes as 1) "*exclusive delivery*" of uranium, cesium, and iodine to the Earth by aliens, 2) the massive star explosion due to "*over-saturation by iron and nickel*", 3) the null-impulse "*teleportation*" of elements at dying low-mass stars. Due to implausible mistakes, we regretfully ascertain that the theory of terrestrial ore origin is absent. Note most of the opponent's responses have the main goal not to find the truth but to annoy the author. Especially for angry opponents, the simplest textbook transfer task is given in the **Appendix**. This task has no solution within the frame of up-to-date astrophysics.

Further, as it is known, the stellar abundance is defined by local synthesis, called a self-enriched process, transferring elements from other remote stars. These two processes can be written by Equations (1) and (2):

$$A_{star} = A^s_{star}\left(t_e\right) + A_T\left(t_e, t_T\right) \tag{1}$$

$$A_T\left(t_e, t_T\right) = \sum_{i=1}^{n} \alpha\left(t_T\right) \cdot A_i\left(t_e\right) \tag{2}$$

where A_{star} is actual abundance, A^s_{star} —the self-enriched process at star evolution, A_T —the elements, obtained from remote stars, and $\alpha\left(t_T\right)$ is space scattering coefficient.

According to the older B^{2}FH model [3] and the newest K^{2}L models [16], necessary elements for life origin, are synthesized on different stars, in other words $A_T \gg A^s_{star}$. It is essential to notice that the synthesis of various elements on different stars made it impossible to raise biological forms on these stars.

In a previous work [17], this problem was solved by the self-enriched process, *i.e.*, the first term in the Equation (3) prevails, ($A_T \ll A^s_{star}$). Thus the Equations

(3) and (4) can be rewritten as:

$$A_{star} = A^{s}_{star}\left(t_e\right) + A_T\left(t_e, t_T\right) \approx A^{s}_{star}\left(t_e\right) \tag{3}$$

$$G = G\left(x, y, z, t_e\right) \tag{4}$$

where x, y, z are galaxy spatial coordinates and G is the gravity in the studied area of the Milky Way Galaxy.

Due to the long duration of evolution, it is impossible to observe stellar developments, therefore in our study new approach consisting in the study properties of the Ensemble-Averaged Stellar Reactor (EASR) is applied. In the assumption that stellar evolution occurs under the influence of galaxy gravity, we replace the analytical decision of system of the Equations (3) and (4) with the investigation of spatial distributions:

$$A^{s}_{star} = A^{s}_{star}\left(x, y, z\right) \tag{5}$$

After reading [17], the reader already knew that in addition to well-known processes of slow neutron capture (s-process) and rapid neutron capture (r-process), there is a new synthesis process in the overheated stars (h-process). The goal of this study is to find an answer to the following question: Where in the solar neighbourhood are these overheated stars?

2. Materials and Methods

2.1. Stellar Abundances in the Solar Neighborhood

The stellar abundances in the solar neighborhood are accessible on the site of Hypatia Stellar Catalog (below HSC) by [18]. This dataset includes stellar names, spectral type, distance from Sun, position, and the elemental abundances for stars in ~200 pc solar neighborhood. The database is updated continuously; currently, it contains information about 3757 stars and about 43 chemical elements. Note that the number of chemical elements registered in the spectra of stars and presented in the HSC dataset may differ for different stars. A detailed description of these data can be found in [19] [20]. Based on the HSC data, a spatial analysis of the distribution of elements in this part of the galaxy was carried out.

2.2. Rates of Element Synthesis

As it is well known, a nuclear reactor produces heat and chemical elements, so that the reactor's state can be evaluated by abundance and temperature. In this study, element synthesis (degradation) rates were obtained as bias at the linear regression in functional dependence between element abundances and effective stellar temperature (below AT diagram). In the HSC catalog, the abundance of chemical elements is defined as the deviation from the distribution in the Sun, normalized according to data of [21] and referred to the H content. Therefore the stellar abundances are measured in relative units [element/H] looks like:

$$\log\left(n_{\text{element}}/n_{\text{H}}\right)\left(\text{star}\right) - \log\left(n_{\text{element}}/n_{\text{H}}\right)\left(\text{solar}\right)$$

and the unit of element synthesis rate is K^{-1}. The resulting tables will show the

correlation coefficient (R) and standard deviation (SD) in AT diagrams. The resulting tables will include only statistically significant values with $|R| > 0.12$ and amount stars N more than 10 ($N > 10$).

2.3. The Ensemble-Averaged Stellar Reactor

Both models, the oldest B^2FH and the newest K^2L, are hypothetical. In this study new model was developed, but this model was based not on abstract theoretical concepts but on the spectral data available to the author.

We cannot have the possibility to scan the change of an individual stellar reactor in the range of billions of years; therefore, in our study, we forced to use the averaging over the ensemble of all HSC stars and investigate the operating characteristics of a hypothetical ensemble-averaged reactor. The novelty of this approach is consists in that the star ceases to be a static nuclear object. This new model is called the ensemble-averaged stellar reactor model (below EASR model).

2.4. The Working Cycles of Ensemble-Averaged Stellar Reactor

The ensemble-averaged stellar reactor (EASR) is a generalized thermal nuclear engine that provides the generation of heat and the variety of chemical elements in the universe. Therefore, it is convenient to represent the dynamics of the ensemble-averaged stellar reactor working in the stellar Radius and stellar effective Temperature coordinates, below RT.

The dependence of the stellar radii on the effective temperature is shown in Figure 1. The directions of operation of such a thermal nuclear engine are indicated in the figure by arrows. The distribution of HSC stars in the RT diagram combines linear and exponential distributions, drawing by red and blue lines in Figure 1, respectively. The empirical formulas for these distributions are defined by the expressions Equation (6) and (7):

$$R_{red} = \alpha + \beta T \tag{6}$$

$$R_{blue} = \chi \mathrm{e}^{-\gamma T} \tag{7}$$

where $\alpha = 2$, $\beta = 6 \times 10^{-4}$ and $\chi = 12.86 \times 10^5$, $\gamma = 1/400$.

Based on the distribution presented in Figure 1 it was possible to allocate in RT diagram four stellar classes, called as RT1-RT4. The statistical distributions of HSC stellar radius measured in the size of solar radius ($R_\odot$) and the effective stellar temperature were presented in Table 1. The range of 5200 - 5600 K, where mixed processes dominate, was not considered in this work.

In the proposed approach, the stellar mass is not the deciding parameter, so just for comparison, we note that at T = 6500 K, $R \sim 1.9 R_\odot$ and stellar masses were in the range: $M \sim 1.33\text{-}1.38 M_\odot$. In the RT3 site, the stellar-mass reached a maximum value $M \sim 1.76 M_\odot$ at 7362 K.

The explosive processes of star expansion are indicated in the RT diagram by green lines. These processes occur quickly, so the number of measured values is not sufficient to determine the parameters of the generalized reactor in the area

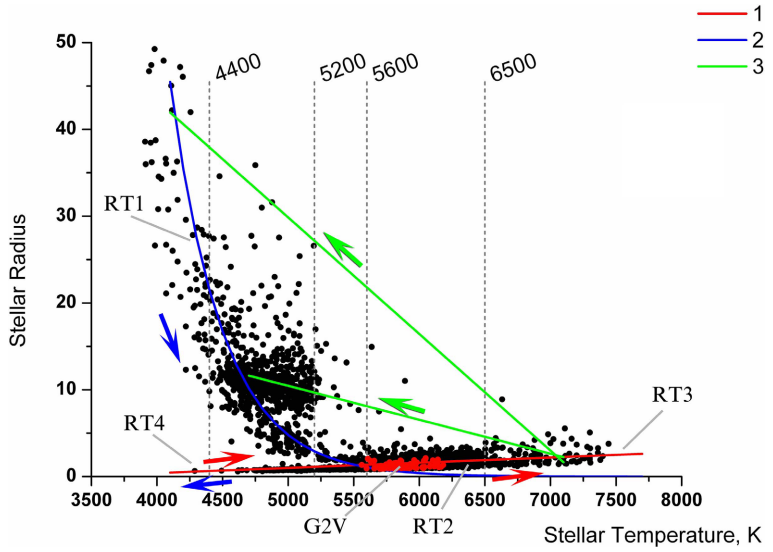

Figure 1. The scheme of working of the thermal nuclear engine, which is providing generation of heat and a variety of chemical elements in the Universe, it is designated by arrows (1-2-3). The stars from Hypatia Stellar Catalog (HSC), belonging to the G2V spectral class, are drawn as red points. The studying ranges were marked as RT1-RT4 sites.

Table 1. The investigation ranges in the RT charts. The T is the effective stellar temperature, R_s—HSC stellar radius and $R_\odot$—solar radius.

Name	Description	Amount of stars	
		pcs.	%
RT1	$4400 < T < 5200$ K; $R_s > 2R_\odot$	859	27.0
RT2	$5600 < T < 6500$ K	1989	62.6
RT3	$T > 6500$ K	136	4.3
RT4	$4400 < T < 5200$ K; $R_s < 2R_\odot$	192	6.0
	Total	3176	100

between RT3 and RT2. In the course of calculations, the site of explosive rapid star expansions was not used, and therefore, it does not have a special designation. Conventionally, the temperature corresponding to 7100 K is chosen as the starting point of this explosive site, which in the RT diagram corresponds to $R \sim 2.2R_\odot$ and $M \sim 1.58M_\odot$. Further, the stars, located between RT1 and RT2 sites (5200 - 5600 K), for which it is not possible to separate the processes, were also excluded from consideration.

Let's result in a general characteristic of work such hypothetical the thermal engine. The main process of operation of the heat nuclear engine of the EASR reactor is RT1-RT2-RT3 process. This process is unidirectional, since it is a process of heating, exploding, and expanding the star and its compression with the gradual restoration of the stellar reactor working state. On the other hand, in the RT4 linear site, EASR reactor can operate in both directions, both at new star birthing and at low-mass star dying.

2.5. The Nuclear Binding Energy and Syntheses of Transuranium Elements

Because the maximum of nuclear binding energy occurs near ^{56}Fe, stars cannot get energy by nuclear fusion and stellar nucleosynthesis come to a stop on ^{56}Fe. The dependents average binding energy per nucleon versus the atomic number is presented in **Figure 2(a)**, *i.e.* (B/A vs. Z), where B is binding energy, A—number of nucleons (mass number), and Z—the atomic number. In **Figure 2(a)**, the experimental data are presented as dots. Note that these experimental data were obtained in the laboratory conditions, *i.e.*, during experiments on accelerators, cyclotron, or reactors.

As it is well known, the experimental curve presented in **Figure 2(a)** contains fusion exothermic (before ^{56}Fe) and fusion endothermic (beyond ^{56}Fe) parts. In theory, the simulated curve of binding energy $B(A, Z)$ is given by using the following formula [22]:

$$B(A,Z)=\alpha_v A+\alpha_s A^{2/3}+\alpha_c Z(Z-1)A^{-1/3}-\frac{\alpha_{asym}(A-2Z)^2}{A}+\delta\alpha_p A^{-3/4} \quad (8)$$

where Z—number of protons; N—number of neutrons; A—is the mass number. This Equation has 5 terms corresponding to volume, surface, Coulomb, asymmetric and pairing terms. The constants of these terms are fitting parameters that are found experimentally to be equal to next: $\alpha_n = 15.5$ MeV, $\alpha_s \sim 18$ MeV, $\alpha_c = 0.691$ MeV, $\alpha_{asym} = 23$ MeV.

The details about Liquid Drop Model (LDM), discussion about other binding models, and references could be found, e.g., in [23] [24]. Note that the fourth term in Equation (8) is an asymmetry term in which it is taken into account the asymmetry in protons and neutrons. The excess of neutrons over protons is drawn in **Figure 2(b)**.

The gray curve presented in **Figure 2(a)** is related to result obtained in a vacuum on accelerators or in scientific reactors. However, note that the conditions on stars are different from laboratory conditions, so in stars the binding energy curve per nucleon can be propagated above the horizontal discontinuous line (~8.8 MeV) in **Figure 2(a)**, then all the elements of the periodic table were synthesized. Moreover, if the curve is above this line, then there would be a constant synthesis of Th and U atoms, and the star is going to extra saturate by nuclear fuels.

Hence, exactly asymmetry term, which considers the difference in the number of neutrons and protons in the element, causes that synthesis of elements will stop at Fe. Therefore asymmetry is responsible for the fact that the core of a regular star, which has not undergone explosive transformations, is iron-nickel core. However, at present, in astrophysics, it is assumed that only the pre-collapsed, massive star with mass $M > 10M_{\odot}$, where $M_{\odot}$ is the mass of Sun, has an iron-nickel core.

Thus, it is possible to assume that, under galaxy load the atomic nucleus lose neutrons and an excess of neutrons over protons is leveled; see **Figure 3**. Such

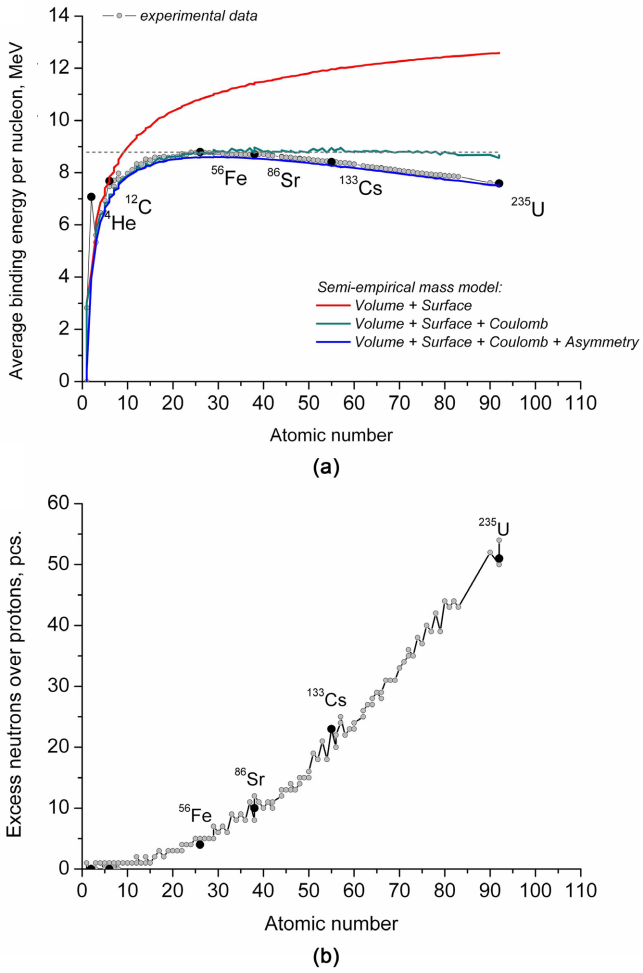

Figure 2. (a) The nuclear binding energy per nucleon for stable nuclei in terms of mass number was presented by points (B/A vs Z). The experimental values were presented by points. The comparison between the result of the LDM model, in which it was taking into account the different model terms (color lines) and the experimental values were shown; (b) Excess netrons over protons.

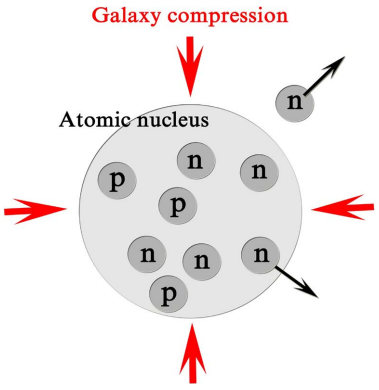

Figure 3. The simple scheme of emission of neutrons under the pressure of a galaxy, leading to displacement endothermic limit aside to heavier elements and synthesis of transuranium elements. At last at the galaxy compression the star becomes the neutron star (NS).

process gives the chance displacement fusion endothermic limit aside to heavier elements.

The accumulation of transuranic elements inside a star can occur, firstly leading to the heating of the stars and secondary it leads to that the star to emit overstock neutrons into space and the star evolves into the neutron star. At reaching the threshold values of uranium, the star explodes and collapses. Note that before this study, there is no physical explanation for the Chandrasekhar mass limit $M_{Ch} \sim 1.44 M_{\odot}$.

At last, it is important to note that the binging model (Equation (3)) and experimental values, presented in Figure 4(a), apply to the individual atomic nucleus, that is, for a case when a star or planet can be represented as an ideal gas or rarefied plasma. Thus, basically, the binding theory is not applicable to the non-equilibrium plasma of which mostly overheated stars are composed.

3. Syntheses of Heavy Elements

3.1. Stellar Nucleosynthesis on Cold Stars

In the EASR reactor, the synthesis process is called a process at which the element abundance increases at increase in the effective stellar temperature. In consideration, it included only statistically significant values with $R > 0.12$ and amount stars more than 10, $N > 10$. Here the R is the correlation coefficient on AT diagram between abundance and effective stellar temperature.

The amount of synthesized elements increases in the RT1-RT2-RT3 cycle and it reaches 14 pcs for hot RT2 stars and 28 pcs for RT3 overheated RT4 stellar group.

The elements synthesised in the cold RT1 and RT4 stellar group are presented in Table 2 and Table 3. Remind that in Tables the bias is the slope between abundance and effective temperature; the SD is the standard deviation; N—number of stars in statistical sampling; R_s is stellar radius and $R_{\odot}$ —solar radius, and "*II*" is a label which corresponds to the ionization state of an element.

3.2. Stellar Nucleosynthesis on Hot and Overheated Stars

The elements, which were synthesized on hot and overheated stars are presented in Table 4 and Table 5.

Actually, there is an increase in amounts of the element, which saturation grows with effective stellar temperature. However, syntheses of Fe and Ni are recorded only in the overheat RT3 stars Table 5. The carbon (C) is observed on the RT3-RT1 degradation branch, *i.e.* at the negative bias at AT diagram. Similarly, in the EASR model the oxygen (O) is recorded in the degradation branch in the spectrums of the post-explosive RT1 stars and the cold RT4 stars. The phosphorus (P) degradation was found only in the hot RT2 stellar group. Note that negative biases are not presented in Tables 3-5.

Two sites have dropped out of our consideration, namely site between RT1 and RT2 groups at 5200 - 5600 K, for which it is not possible to separate stellar

Table 2. The elements synthesised in cold RT4 stellar group.

RT4 stellar group (192 stars)					
$4400 < T < 5200$ K, $R_s < 2R_\odot$ Bias > 0, $R > 0.12$ and $N > 10$					
		$10^4 \times$ bias	R	SD	N
1	Li	16.80	0.262	0.813	57
2	N	6.72	0.295	0.252	53
Fe-Ni endothermic level					
3	Zr	1.82	0.120	0.213	171
Lanthanides					
4	Eu	4.23	0.305	0.200	65

Table 3. The elements synthesised in the post-explosive RT1 stellar group.

RT1 stellar group (859 stars)					
$4400 < T < 5200$ K, $R_s > 2R_\odot$ Bias > 0, $R > 0.12$ and $N > 10$					
		$10^4 \times$ bias	R	SD	N
1	Li	8.91	0.322	0.489	766
2	Be_{II}	20.30	0.500	0.396	57
3	K	6.76	0.470	0.162	148
Fe-Ni endothermic level					
4	Sr	1.59	0.162	0.181	785
5	Zr	2.59	0.214	0.222	804
6	Ba_{II}	4.10	0.333	0.217	811
7	Hf	13.00	0.642	0.199	40
Lanthanides					
8	Ce	1.90	0.154	0.214	259
9	Gd_{II}	4.39	0.184	0.321	48

Table 4. The elements, which were synthesised in hot RT2 stellar group.

RT2 stellar group (1989 stars)					
$5600 < T < 6500$ K Bias > 0, $R > 0.12$ and $N > 10$					
		$10^4 \times$ bias	R	SD	N
1	Li	18.20	0.555	0.548	1035
2	Be	8.46	0.377	0.515	10
Fe-Ni endothermic level					
3	Y	3.18	0.216	0.326	1187
4	Zr	5.71	0.350	0.340	1160

Continued

5	Mo	6.30	0.289	0.253	34
6	Pd	7.85	0.498	0.244	36
7	Ag	10.20	0.582	0.253	36
8	Ba	4.95	0.532	0.214	13
		Lanthanides			
9	La	2.60	0.182	0.383	34
10	La_{II}	3.46	0.258	0.287	1024
11	Ce	4.63	0.346	0.302	50
12	Nd	3.02	0.213	0.327	93
13	Sm	3.86	0.301	0.343	31
14	Eu	4.36	0.178	0.467	374

Table 5. The elements, which were synthesised in the overheated RT3 stellar group.

RT3 stellar group (136 stars)					
$T > 6500$ K Bias $> 0, R > 0.12$ and $N > 10$					
		$10^4 \times$ bias	R	SD	N
1	Li	7.07	0.234	0.727	23
2	N	4.83	0.352	0.354	15
3	Na	4.15	0.420	0.254	132
4	Mg	1.34	0.188	0.198	129
5	Al	3.06	0.301	0.245	101
6	Si	1.58	0.251	0.173	132
7	S	2.33	0.262	0.242	132
8	K	6.57	0.355	0.333	16
9	Ti_{II}	1.87	0.217	0.258	66
10	V	5.21	0.431	0.309	115
11	Cr_{II}	2.52	0.333	0.217	66
12	Mn	2.74	0.291	0.253	124
13	Fe	1.73	0.220	0.213	131
14	Co	6.53	0.454	0.332	112
15	Ni	2.05	0.224	0.251	134
		Fe-Ni endothermic level			
16	Cu	6.85	0.455	0.368	98
17	Zn	4.55	0.389	0.307	115
18	Sr_{II}	8.84	0.548	0.392	24
19	Y	3.11	0.174	0.458	80
20	Y_{II}	4.07	0.364	0.337	49

Continued

21	Zr_{II}	3.76	0.302	0.385	39
22	Ba	5.90	0.440	0.303	59
23	Ba_{II}	11.30	0.689	0.356	62
		Lanthanides			
24	La	5.74	0.333	0.405	74
25	Ce	6.14	0.433	0.318	71
26	Nd	6.45	0.490	0.291	60
27	Sm	5.37	0.430	0.278	51
28	Eu	5.75	0.245	0.576	62

processes, and second site of the RT3-RT1, draw as green arrows in Figure 1, on which under our assumption the fast explosive processes take place and on which is not enough statistics. Therefore syntheses of C, O, and P it is possible to explain by currently unknown synthesis at star explosions, or by fading of cold stars, *i.e.*, by the reverse way in the RT4 branch. Presence of considerable C and O quantity in the atmospheres of gas giants in our solar system testifies more likely that synthesis occurs during explosive processes. Thus the nature is more intricate and complicated than it is supposed under the elementary scheme presented in Figure 3.

4. Results

As a result of the spatial distribution of element abundances analysis, it was established that the distribution has random scattering behaviors. However, we found interesting features in the spatial distribution of the overheated RT3 stellar group. In the Section 1, we already mentioned the galaxies effect on stars, so the effect was expected, and accordingly, we searched for it. In this section galaxy influence on stars is demonstrated in detail.

The position of the HSC stars is determined in Cartesian geocentric XYZ-coordinates from the Sun and is described by the following relations:

$$\begin{aligned} X &= d \cdot \cos(dec) \cdot \cos(ra) \\ Y &= d \cdot \cos(dec) \cdot \sin(ra) \\ Z &= d \cdot \sin(dec) \end{aligned} \tag{9}$$

where *ra* is right ascension and *dec*—declination from Hipparcos (J2000) and *d*—the distance from Sun in pc.

The Z-cross-section statistical distributions are presented in Figure 4 for RT1-RT4 stellar groups. The RT2 stars have in Z-cross-section symmetric distribution. The number of these stars allocated above the Z = 0 line (931 stars) is approximately equal to the number of stars below the line Z = 0 (1058 stars), Figure 4(b). The stars from RT1 and RT3 stellar groups have distributions shifted upward. However, the greatest interest represents the distribution for overheated stars from the RT3 stellar group, see arrow in Figure 4(c).

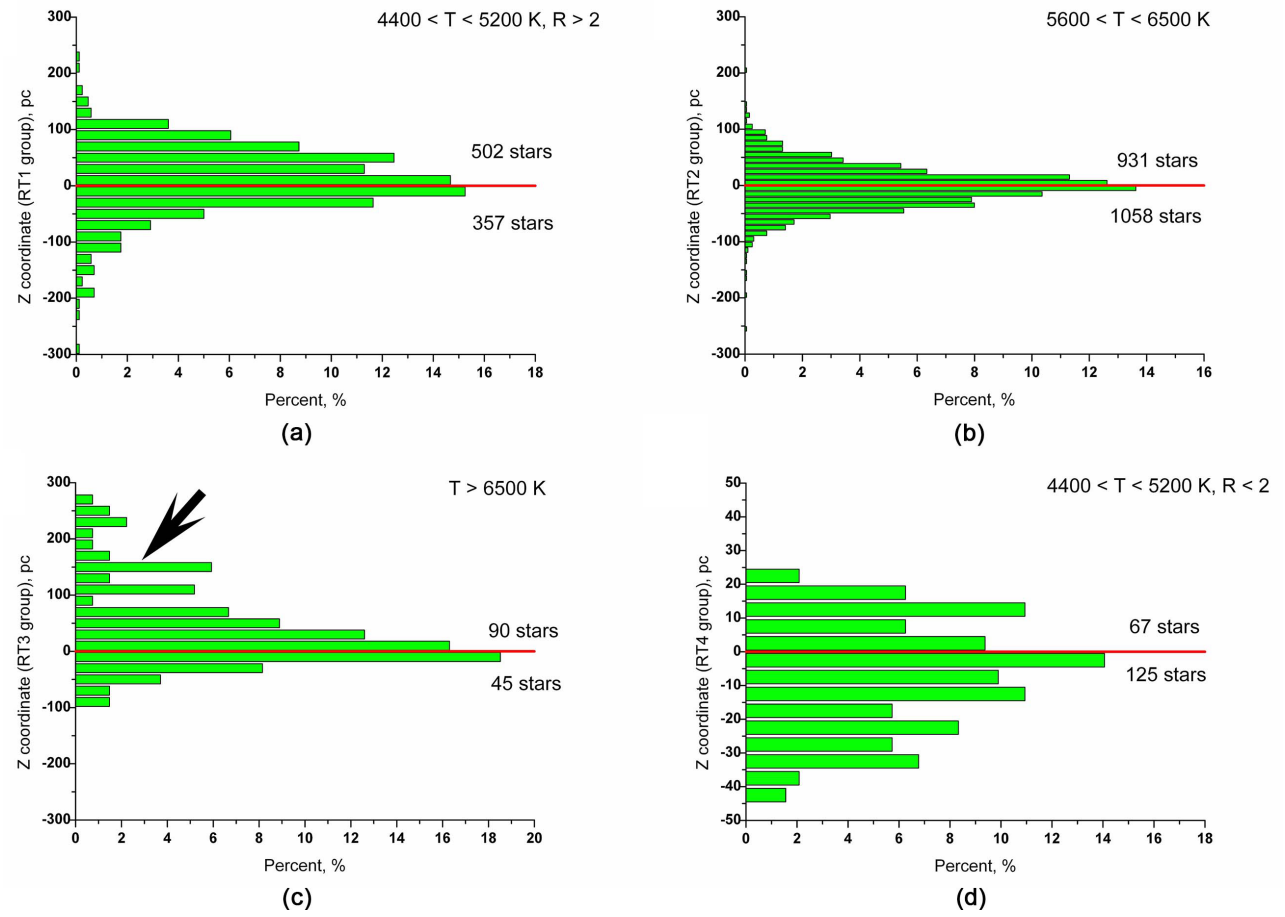

Figure 4. The Z-cross-sections of RT1-RT4 stellar groups were presented. The overheated stars from the RT3 stellar group have strongly pronounced asymmetrical displacement upwards to $Z = 0$; please, see arrow in (c).

The spatial distribution of the RT3 stellar group was presented in **Figure 5** in XYZ coordinates with additional 3D color plane projections. The blue points in Figure are projected on the YZ plane, the red and green points—on XY and XZ planes, respectively. It may seem that the above unusual distribution concerns only the temperature distribution, but same spatial distribution is typical, for example, for the neutral state of lanthanum.

The comparisons of the spatial distribution of "*hot*" and "*cold*" stars from RT3 and RT1 stellar groups in XZ and YZ-coordinates were drawn in **Figure 6**.

For clarity, the RT1 stars that have stellar radius $R > 16R_{\odot}$ are presented in **Figure 6(a)** and **Figure 6(c)**. These stars were presented with an additional color gradation of stellar radius. The stars with a large radius $R > 22R_{\odot}$ are located below level $Z = 0$; see the red and yellow cycles in **Figure 6(a)** and **Figure 6(b)**. However, stars with $16 < R < 20R_{\odot}$ form a local group that looks like a roll, above the level of $Z = 0$. The dotted lines in Figures correspond to the harmonic sinusoid approximation.

The spatial distributions, presented in **Figure 5** and **Figure 6**, show that the operation of a generalized, EASR reactor has not only a pronounced temperature range but is also determined by the spatial distribution of stars in the galaxy.

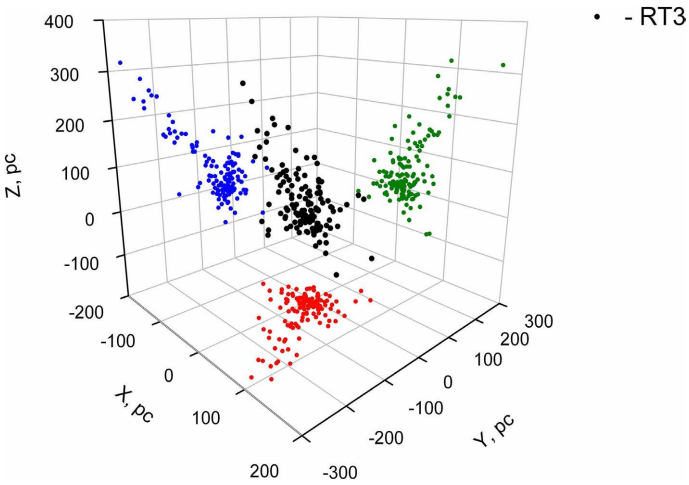

Figure 5. The spatial distribution of "*hot*" stars from RT3 stellar group, but in Cartesian geocentric XYZ-coordinates with additional color plane projections. Blue points are projected on YZ, red points—on XY, and green—on XZ planes.

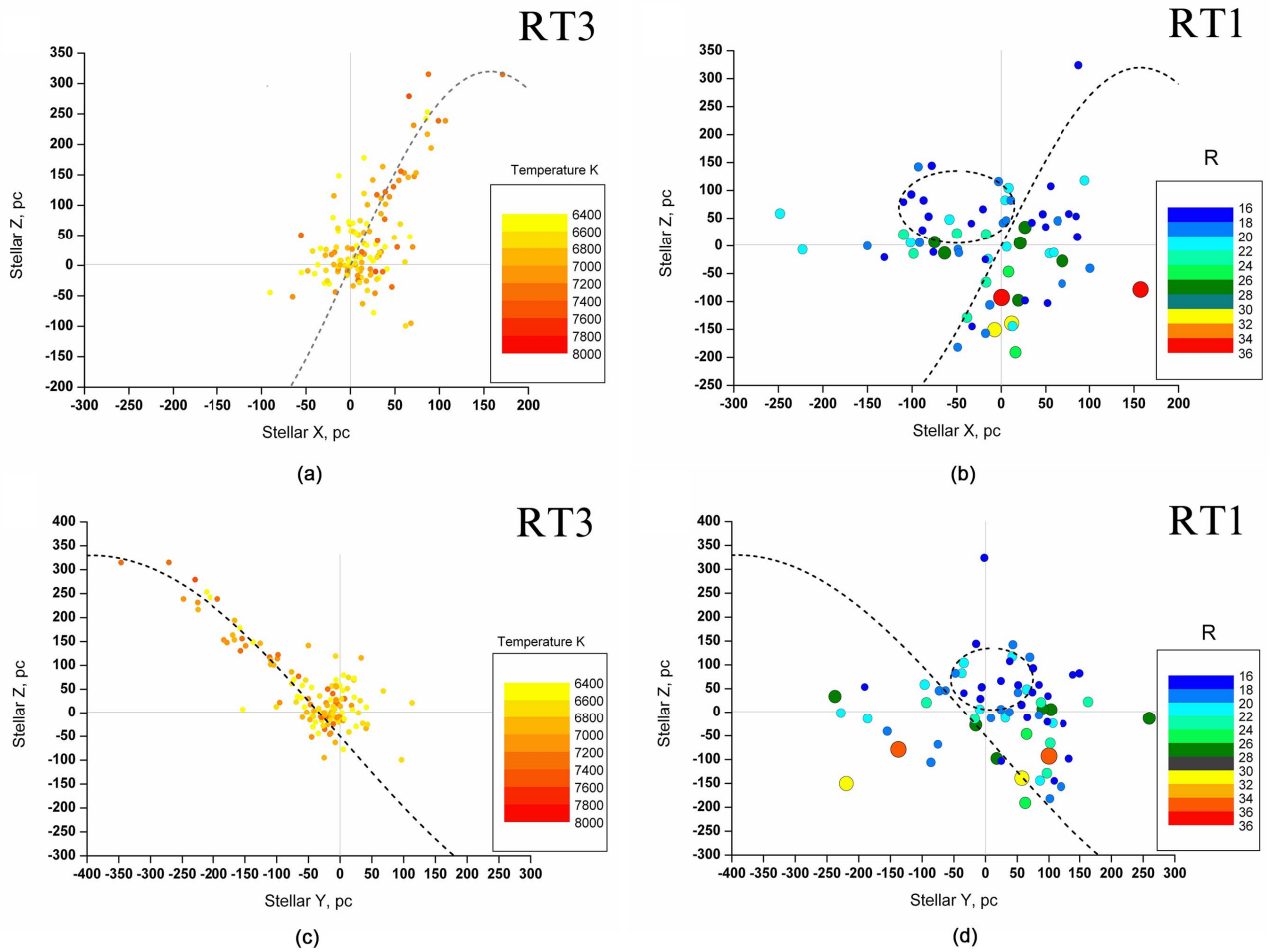

Figure 6. (a) Spatial distribution of RT3 stars in Cartesian geocentric XZ-coordinate system with additional temperature color gradation at $T > 6500$ K ; (b) Spatial distribution of RT1 stellar group in XZ-coordinate system with additional color gradation at stellar radius $R > 16R_{\odot}$. In (c) and (d) similar spatial distributions were presented but in the YZ-coordinate system.

Thus it is possible to come out with the careful assumption that the withdrawal of the star from the equilibrium state is a result of galactic compression within the galactic arm due to the spirality of the arm. Still, this question is far beyond the scope of this publication. Note that any internal structure of the galaxy, which does not fit into the framework of general relativity, is undoubtedly a surprise for Einstein's followers. From **Figure 6** the question about the balance of mass on the external border of a Milky Way Galaxy immediately arises. The synthesis of elements from a vacuum, which it is possible to name as "*vacuum quantization*", raises doubts.

5. Discussion and Some Remarks

After the 2011 disaster at the Fukushima Daiichi Nuclear Power Plant, the International Atomic Energy Agency (IAEA) initialized testing reactors, primarily industrial and scientific reactors. However, then this process was expanded to the natural reactors. In 2013, it was reported about problems in nuclear geophysics.

Now it is very difficult to believe that the geoneutrino researchers did not know about the threshold of observability of neutrino spectra, the differentiation of heavy elements in magmatic layers, and the non-uniformity distributions of Th and U in the old faults of the lithosphere. The gross error in the observability threshold of the neutrino spectrum does not give a chance to predict the presence of a hot fuel ^{40}K nuclear layer at a depth of 660 km. Without data about nuclear processes inside the Earth occurred at the boundary of the upper and lower mantle, it is impossible to create a modern theory of volcanic eruptions, predictions of earthquakes and explain subduction processes.

Note that the theory of the formation of the ore, which was raised from the depths of the Earth and stuck in the old faults can be generalized to the theory of the ore formation on other solar planets; in particular, it can be used into an investigation of ores on Mars.

The implausible mistake of the geoneutrino groups caused serious loss to geophysics and set geophysics back for several decades. Note that early in [25] and [26] it was shown that the ^{40}K thermal nuclear layer, which can be called a *hell's frying pan* or a thermal nuclear bomb, is located at a depth of 660 km, on the borders of the upper and lower mantle. This ^{40}K fuel layer is the basis of new volcanology and seismology theories, subduction, continental drift and ores original. After geophysics, it has come the turn of nuclear astrophysics. Unfortunately, the Author is obliged to report that nuclear astrophysics does not pass the stress test. Raised the question about a terrestial uranium origin, the author sends a couple of hundred GCE publications in highly rated journals to the trash in several seconds. Once again remind that the simplest textbook transfer task, which is presented in the **Appendix**, does not have solution within the frame of up-to-date astrophysics. Such defects as "*exclusive delivery*" of uranium, cesium and iodine to the Earth by aliens, the massive star explosion due to "*over-saturation by iron and nickel*", the null-impulse "*teleportation*" of elements at dying

low-mass stars, "*vacuum quantization*" are absolutely unacceptable for scientific views.

6. Conclusions

The spatial distribution of the abundances in the spectrums of HSC stars showed the chaotic nature of the spatial distribution. It was proved that spatial distribution of elements does not confirm the correctness of the B^2FH and K^2L synthesized models, which a priori state that all elements heavier than iron should be synthesized on stars during the s- and r-processes. In the absence of interstellar transfer of heavy elements, in addition to s- and r-processes, one more self-enriched stellar mechanism must exist. This study found that it is a synthesis of elements on the hot stars with $T > 6500\,\mathrm{K}$. This new process can be called an h-process.

It was assumed that the ensemble-averaged stellar reactors (EASR) have a common K-Sr-Cs-Pb-Th-U multilayer structure. Also, it is suggested that stars warming up due to the displacement of the nuclear processes occurring inside the stars, which leads to the synthesis of transuranic elements, to an accumulation of a critical nuclear mass, and at the end to star explosion. In this study for the first time a physical explanation of the existence of the critical Chandrasekhar star limit has been offered.

The detailed analysis of the spatial distribution of overheated stars with an effective stellar temperature of more than 6500 K was carried out. Based on the analysis, it was shown that the withdrawal of the stellar reactor from the equilibrium state is a consequence of extra galactic compression inside the galaxy arm due to the arm spirality (not to be confused with the spirality of the galaxy itself).

Acknowledgements

We would like to thank *N. R. Hinkel*, *F. X. Timmes*, *P. A. Young*, *M. D. Pagano*, *M. C. Turnbull* for providing valuable and useful Hypatia Stellar Catalog. Also sincerely thanks to the members of JHEPGC for their professional performance, and special thanks to managing editor Ms. Zoey Yang attitude of high quality.

Conflicts of Interest

The author declares no conflict of interest.

References

[1] Hoyle, F. (1946) The Synthesis of the Elements from Hydrogen. *Monthly Notices of the Royal Astronomical Society*, **106**, 343-383. https://doi.org/10.1093/mnras/106.5.343

[2] Hoyle, F. (1954) On Nuclear Reactions Occurring in Very Hot STARS. I. The Synthesis of Elements from Carbon to Nickel. *Astrophysical Journal*, **1**, Article No. 121. https://doi.org/10.1086/190005

[3] Burbidge, E.M., Burbidge, G.R., Fowler, W.A. and Hoyle, F. (1957) Synthesis of the Elements in Stars. *Reviews of Modern Physics*, **29**, 547-650.

https://doi.org/10.1103/RevModPhys.29.547

[4] Cameron, A.G.W. (1957) Stellar Evolution, Nuclear Astrophysics, and Nucleogenesis. Atomic Energy of Canada, Report CRL-41. https://fas.org/sgp/eprint/CRL-41.pdf

[5] Clayton, D.D., Fowler, W.A., Hull, T.E. and Zimmerman, B.A. (1961) Neutron Capture Chains in Heavy Element Synthesis. *Annals of Physics*, **12**, 331-408. https://doi.org/10.1016/0003-4916(61)90067-7

[6] Seeger, P.A., Fowler, W.A. and Clayton, D.D. (1965) Nucleosynthesis of Heavy Elements by Neutron Capture. *The Astrophysical Journal*, **11**, 121-126. https://doi.org/10.1086/190111

[7] Viola, V.E. (1990) Formation of the Chemical Elements and the Evolution of Our Universe. *Journal Chemical Education*, **67**, 723-730. https://doi.org/10.1021/ed067p723

[8] Jonson, B. (1995) Nuclear Processes in Astrophysics. *Physica Scripta*, **T59**, 53-58. https://doi.org/10.1088/0031-8949/1995/T59/006

[9] Wallerstein, G., Iben, I., Parker, P., Boesgaard, A.M., Hale, G.M., Champagne, A.E., Barnes, C.A., Kappeler, F., Smith, V.V., Hoffman, R.D., Timmes, F.X., Sneden, C., Boyd, R.N., Meyer, B.S. and Lambert, D.L. (1997) Synthesis of the Elements in Stars: Forty Years of Progress. *Reviews of Modern Physics*, **69**, 995-1084. https://doi.org/10.1103/RevModPhys.69.995

[10] Travaglio, C., Gallino, R., Arnone, E., Cowan, J., Jordan, F. and Sneden, C. (2004) Galactic Evolution of Sr, Y, and Zr: A Multiplicity of Nucleosynthetic Processes. *The Astrophysical Journal*, **601**, 864-884. https://doi.org/10.1086/380507

[11] Reifarth, R., Lederer, C. and Kappeler, F. (2014) Neutron Reactions in Astrophysics. *Journal of Physics G, Nuclear and Particle Physics*, **41**, Article ID: 053101. https://doi.org/10.1088/0954-3899/41/5/053101

[12] Goriely, S. and Pinedo, G.M. (2015) The Production of Transuranium Elements by the r-Process Nucleosynthesis. *Nuclear Physics A*, **944**, 158-176. https://doi.org/10.1016/j.nuclphysa.2015.07.020

[13] Liccardo, V., Malheiro, M., Hussein, M.S., Carlson, B.V. and Frederico, T. (2018) Nuclear Processes in Astrophysics: Recent Progress. *The European Physical Journal A*, **54**, Article No. 221. https://doi.org/10.1140/epja/i2018-12648-5

[14] Prantzos, N., Abia, C., Limongi, M., Chieffi, A. and Cristallo, S. (2018) Chemical Evolution with Rotating Massive Star Yields. I. The Solar Neighbourhood and the s-Process Elements. *Monthly Notices of the Royal Astronomical Society*, **476**, 3432-3459. https://doi.org/10.1093/mnras/sty316

[15] Karakas, A.I. (2018) Nucleosynthesis in Stars: The Origin of the Heaviest Elements. *Proceedings of the International Astronomical Union*, **14**, 79-88. https://doi.org/10.1017/S1743921318006166

[16] Kobayashi, C., Karakas, A.I. and Lugaro, M. (2020) The Origin of Elements from Carbon to Uranium. *The Astrophysical Journal*, **900**, Article No. 179. https://doi.org/10.3847/1538-4357/abae65

[17] Safronov, A.N. (2023) Life Origin in the Milky Way Galaxy: I. The Stellar Nucleogenesis of Elements Necessary for the Life Origin. https://doi.org/10.20944/preprints202305.0202.v1

[18] Hinkel, N.R., Timmes, F.X., Youngm P.A., Pagano, M.D. and Turnbull, M.C. (2020) Dataset: Stellar Abundances in the Solar Neighborhood: The Hypatia Catalog. https://www.hypatiacatalog.com/hypatia/default/launch

[19] Hinkel, N.R., Timmes, F.X., Young, P.A., Pagano, M.D. and Turnbull, M.C. (2014) Stellar Abundances in the Solar Neighborhood: The Hypatia Catalog. *The Astronomical Journal*, **148**, Article No. 54. https://doi.org/10.1088/0004-6256/148/3/54

[20] Hinkel, N.R., Young, P.A., Pagano, M.D., Desch, S.J., Anbar, A.D., Adibekyan, V., Blanco-Cuaresma, S., Carlberg, J.K., Mena, E.D., Liu, F., Nordlander, T., Sousa, S.G., Korn, A., Gruyters, P., Heiter, U., Jofr, P., Santos, N.C. and Soubiran, C. (2016) A Comparison of Stellar Elemental Abundance Techniques and Measurements. *The Astrophysical Journal Supplement Series*, **226**, Article 4. https://doi.org/10.3847/0067-0049/226/1/4

[21] Lodders, K. (2010) Solar System Abundances of the Elements. In: Goswami, A. and Eswar Reddy, B., Eds., *Principles and Perspectives in Cosmochemistry*, Springer-Verlag, Berlin, 379-417. https://doi.org/10.1007/978-3-642-10352-0_8

[22] Bohr, N. and Wheeler, J.A. (1939) The Mechanism of Nuclear Fission. *Physical Review D*, **56**, 426-450. https://doi.org/10.1103/PhysRev.56.426

[23] Ghahramany, N., Gharaati, S., Ghanaatian, M. and Hora, H. (2011) New Scheme of Nuclide and Nuclear Binding Energy from Quark-Like Model. *Iranian Journal of Science and Technology*, **A3**, 201-208.

[24] Ghahramany, N., Gharaati, S. and Ghanaatian, M. (2012) New Approach to Nuclear Binding Energy in Integrated Nuclear Model. *Journal of Theoretical and Applied Physics*, **6**, Article No. 3. https://doi.org/10.1186/2251-7235-6-3

[25] Safronov, A.N. (2016) The Basic Principles of Creation of Habitable Planets around Stars in the Milky Way Galaxy. *International Journal of Astronomy and Astrophysics*, **6**, 512-554. https://doi.org/10.4236/ijaa.2016.64039

[26] Safronov, A.N. (2020) A New View of the Mass Extinctions and the Worldwide Floods. *International Journal of Geosciences*, **11**, 251-287. https://doi.org/10.4236/ijg.2020.114014

Appendix

The simple task for GCE models verifications:

The solar reactor is weak and can synthesize mainly hydrogen and helium. According to B^2FH and K^2L models, the thorium can be synthesized in neutron stars (NS), which have a strong reactor. The nearest NS is RX J1856.5-3754, which is allocated at 167 pc from Sun. In the solar system was recorded 1 gram of thorium.

Question: How much of thorium has produced the NS donor-star?